32. EFFECTS OF PLANFORM VARIATIONS ON THE AERODYNAMIC CHARACTERISTICS OF LOW-ASPECT-RATIO WINGS WITH CRANKED LEADING EDGES

By Edward J. Hopkins, Raymond M. Hicks,
and Ralph L. Carmichael
NASA Ames Research Center

SUMMARY

Experimental lift, drag, and pitching-moment characteristics are presented for several wing-body combinations having low-aspect-ratio wings with cranked leading edges. The Mach number range covered was from 0.4 to 2.94. Comparisons are made, throughout this Mach number range, between the measured results and those predicted by means of linear theory in which body induced effects are considered. At a Mach number of 0.4, the effects of changes in the leading-edge crank geometry on the linearity of the lift and pitching-moment curves are shown. At small angles of attack, variations with Mach number of lift-curve slope, aerodynamic center, drag due to lift, minimum drag, and maximum lift-drag ratio are presented.

Some of the benefits of using planforms with cranked leading edges instead of straight leading edges are shown. These benefits include (a) a smaller change in aerodynamic center between subsonic and high supersonic Mach numbers, (b) more usable volume yet less minimum drag for the same exposed area and thickness in percent chord, (c) considerably higher lift-drag ratios at high supersonic Mach numbers for some planar wings, and (d) greater theoretical potential for improvements in flight efficiency by warping. At a Mach number of 0.4, however, the cranked planforms exhibited a loss in longitudinal stability which was more severe than that for the delta planform.

INTRODUCTION

In order for airplanes to meet the stringent range-payload requirement for economic operation at high supersonic speeds, their aerodynamic efficiencies must be maximized at cruise Mach number within the restraints imposed by the overall flight requirements. The optimum design of supersonic airplanes therefore involves many compromises and trade-offs, both aerodynamically and structurally. For example, the most efficient design for supersonic flight may have unacceptable low-speed characteristics or may impose serious weight penalties for maintaining structural integrity. In addition, other conditions such as efficiently providing adequate volume or attaining satisfactory center-of-gravity positions for adequate longitudinal stability throughout the Mach number range may have important influences on the final design.

The initial part of the present investigation was reported in reference 1 where it is shown that aerodynamic efficiency of a flat triangular wing is improved by use of spanwise variation of leading-edge sweep, i.e., an "ogee" planform. The cranked planforms having leading edges consisting of two straight lines should have manufacturing advantages over the ogee planforms they approximate. In references 2 and 3 it is demonstrated that, by lengthening the inboard wing chords, it is possible to reduce the zero lift wave drag and to increase the total wing volume. In reference 4 it is pointed out that for two wings having the same area the one with the more slender planform in the stream direction will have less skin-friction drag.

In the present investigation, the effects of changes in the leading-edge crank geometry on the aerodynamic characteristics of several wing-body combinations were investigated. These planforms, hereinafter called cranked planforms, were designed to have subsonic leading edges over the inward part of their spans throughout the supersonic Mach number range of the investigation. Although the present experimental investigation was confined to planar wings, cranked wings with partly subsonic leading edges should show greater improvement in the flight efficiency from warping than wings with entirely supersonic leading edges. Experimental results for two families of cranked planforms, the one having an aspect ratio of 2.2 and the other an aspect ratio of 1.5, are presented throughout a Mach number range from 0.4 to 2.94.

Part of the present investigation was devoted to predicting the lift, drag, and pitching-moment characteristics at small angles of attack where the experimental curves are nearly linear. The composite method for making these predictions included the mutual interference effects between the wing and the body calculated from slender-body concepts.

NOTATION

A_{exp} exposed aspect ratio, $(\text{Exposed span})^2/(\text{Exposed area})$

C_D drag coefficient based on the area of the triangular wing, $\frac{\text{Drag}}{qS}$

C_{D_o} minimum drag coefficient

C_L lift coefficient based on the area of the triangular wing, $\frac{\text{Lift}}{qS}$

$\partial C_L/\partial \alpha$ lift-curve slope measured at $C_L = 0$

C_m pitching-moment coefficient, $\frac{\text{Pitching moment about } \bar{c}/4 \text{ of delta wing}}{qS\bar{c}}$

(For model 7, the moment center was shifted forward the same amount that the intersection point of the wing trailing edge and the body was shifted forward.)

$\partial C_D/\partial C_L^2$ drag-due-to-lift factor

$\partial C_m/\partial C_L$	pitching-moment-curve slope measured at $C_L = 0$
$\bar{c}$	mean aerodynamic chord of triangular wing, 4.218 in.
$(L/D)_{max}$	maximum lift-drag ratio
M	Mach number
q	free-stream dynamic pressure
R	Reynolds number based on the mean aerodynamic chord of triangular wing
S	wing area of triangular wing including area blanketed by the body, 21.75 in.^{2}
α	angle of attack

MODEL DESCRIPTION

Sketches of all the models investigated are shown in figure 1. Models 1 through 4 all had the same exposed span and area; therefore, they had the same exposed aspect ratio ($A_{exp} = 2.2$). Model 1, which is considered the base planform, is a simple delta planform with its leading edge swept back 59°. Models 2, 3, and 4 all have the same tip chords, trailing-edge geometry, and 78° of sweepback on the inboard portions of their spans. These models differ only in the spanwise position of the leading-edge notch and the leading-edge sweeps on the outer portions of their wing spans. Models 5 through 7 are related in having the same aspect ratios and sweepback of 82° on their leading-edge extensions. Model 6 was formed from model 5 by moving the outer portion of its leading edge forward to create a finite tip; the leading-edge notch was moved inward along the wing span to maintain the same exposed area. Both models 5 and 6 have the same exposed spans and areas to give an exposed aspect ratio of 1.5. Model 7 has the same outboard leading-edge and trailing-edge sweep angles and exposed area as model 1; however, on model 7 the wing was moved forward on the body so that the leading-edge extension and the body nose were coincident. The span was reduced to give a total aspect ratio of 1.5. Model 8 was formed from model 1 by adding a leading-edge extension as shown. This extension had a sharp nose and was slab-sided. Model 8 was made geometrically similar to a much larger scale model which had been investigated in the Ames 40- by 80-foot wind tunnel. Models 1 through 8 all had flat wings mounted in the plane of symmetry of a body of revolution which had a Sears-Haack nose. Model 1 and the outer panels of the remaining models had circular-arc profiles with a thickness of 3-percent chord. The inboard portions of the wing spans of models 2 through 7 had round-nosed symmetrical profiles (NACA 0003-1.1 40/1.75) also with a thickness of 3-percent chord.

REDUCTION OF DATA

The measured axial forces used for computing drag were adjusted to correspond to the free-stream static pressure acting on the fuselage base. The minimum drag data are corrected to conditions corresponding to an all turbulent boundary layer by the method presented in appendix A of reference 1. A correction for the slight leading-edge bluntness of the outboard panels also was made to these drag data by the method presented in appendix B of reference 1. Values of maximum lift-drag ratio were computed from the faired values of the drag-due-to-lift factors and the corrected minimum drag coefficients by the following equation: [1]

$$(L/D)_{max} = \frac{1}{2}\sqrt{\frac{1}{(C_{D_o})(\partial C_D/\partial C_L{}^2)_{\alpha>3^o}}} \qquad (1)$$

THEORETICAL METHODS OF ANALYSIS

Subsonic

The lift and pitching moments for a given model were calculated as the summation of the contributions from the individual components: the nose, the wing extending ahead of the leading-edge notch, and the wing panel outboard of the notch. The lift and center of pressure for the body nose were estimated from slender-body concepts given in reference 5. The mutual interference lift between the various parts of the wing and the body was also accounted for by the slender-body theory given in reference 5. Lift and center of pressure on the part of the wings ahead of the notch were computed by the slender-wing theory of reference 6. This theory was also used to estimate the wing-alone lift and center of pressure on the outboard panels of the models which had pointed tips, namely, models 1, 5, and 7. For the wing-alone lift on the wing panels outboard of the notch on all other models, the method of reference 7, which gives results about the same as the Weissinger method (ref. 8) for low-aspect-ratio wings, was employed.

The skin-friction drag was computed from the incompressible skin-friction equation given in reference 9; compressibility was taken into account by the reference-temperature method of reference 10.

In all cases, since the wings were thin and of low aspect ratio, drag due to lift was assumed to be equal to the lift times the angle of attack; hence, no leading-edge thrust was assumed. The drag-due-to-lift factor $(\partial C_D/\partial C_L{}^2)$

---

[1]This procedure was followed to improve the accuracy of the maximum lift-drag ratio, since the drag polars were found to be parabolic only for angles of attack above about 3^o. The minimum drag coefficients were obtained by extrapolating the drag-due-to-lift curve (C_D vs. $C_L{}^2$) to zero lift.

therefore becomes the reciprocal of the lift-curve slope and the maximum lift-drag ratio is given by equation (1).

Supersonic

The wing-body interference effects on the lift were calculated by the method of reference 5. The wing-alone lift and center of pressure were calculated by the method of reference 11. (A similar but alternate method of computing the wing-alone values is given in ref. 12.) Lift and center of pressure for the body nose were calculated by slender-body concepts.

Wave drag for each wing-body combination was computed for an "equivalent" body of revolution by application of the supersonic area rule described in reference 13. After the skin-friction drag given by reference 10 was added to the wave drag, the maximum lift-drag ratio was calculated by equation (1), which sets the drag-due-to-lift factor ($\partial C_D/\partial C_L^2$) equal to the reciprocal of the lift-curve slope.

DISCUSSION OF RESULTS

Reynolds Number Effects

As an aid in interpreting the subsonic results, results obtained in the Ames 2- by 2-foot wind tunnel on small-scale models in the present investigation at a Reynolds number of only 0.9×10^6 are compared in figure 2 with results for two larger scale models of models 1 and 8 which had been investigated in the Ames 40- by 80-foot wind tunnel. It can be seen that, for model 1, Reynolds number had practically no effect on the lift, pitching moment, or drag-due-to-lift curves. For model 8, the lift-curve slope was slightly higher at the higher Reynolds number but the pitching-moment and drag-due-to lift curves were nearly the same. These results indicate that for low-aspect-ratio highly swept wings with relatively sharp-edged profiles, Reynolds number effects are relatively unimportant in studies of planform effects.

Lift

Effects of planform modification on lift at a Mach number of 0.4 are shown for the two families of wings in figure 3. Linear theory, which includes the mutual interference effects between the wing and the body discussed above, is also shown in figure 3. It can be seen that linear theory gives a good estimate of the lift-curve slope at small angles of attack, but considerably underestimates the lift of the cranked planforms at the higher angles of attack because of the nonlinearity of the measured curves. (Predicting the nonlinear part of the curves would involve accounting for the vortex discharge from the wing leading edge and is beyond the scope of this report.) All of the cranked planforms had considerably more nonlinear curves than the delta planform; greater nonlinearity was measured for the lower aspect-ratio wings. This latter effect is well known for wings with straight

leading edges. Below each model is shown the measured angle of attack required to attain a lift coefficient of 0.8. It should be noted that a small leading-edge extension such as for model 2 produced enough nonlinearity in the lift curve to reduce this angle from approximately 17° to 15°, but that the larger leading-edge extensions, as for model 4, increased this angle to about 18°, partly because a larger portion of this wing was acting as a lower aspect-ratio wing with a lower lift-curve slope. The wings of aspect ratio 1.5, with more nonlinear curves than the aspect-ratio-2.2 wings, required about the same or a greater angle of attack for a lift coefficient of 0.8 than the delta wing because of their lower aspect ratio. It is interesting that model 6, which had a smaller leading-edge extension than model 5, had the more nonlinear lift curve, just as model 2 had compared with model 4.

Pitching Moment

Pitching-moment results obtained at a Mach number of 0.4 for the two families of wings are shown in figure 4. It can be seen again that linear theory gives a good estimate of the longitudinal stability at low lift coefficients, but not at the higher lift coefficients where the cranked planforms exhibited a considerable loss in longitudinal stability. The delta wing showed only a slight loss in longitudinal stability at moderate lift coefficients. For the aspect-ratio-2.2 family (models 1 through 4), note that the loss in longitudinal stability became progressively more severe as more of the wing leading edge was extended forward. This same result can be observed by comparing the data for model 6 with that for model 5 which had the greater leading-edge extension.

Effects of Mach Number

The effects of varying Mach number from about 0.4 to 3 on the important aerodynamic parameters of the two families of wings at small angles of attack are shown in figures 5 through 9. At supersonic Mach numbers some of these parameters such as the slopes of the lift and pitching-moment curves will apply over a larger range of angles of attack. On each of these figures estimated values from linear theory are also shown

Pitching-moment-curve slope ($\partial C_m/\partial C_L$).- The maximum travel in the aerodynamic center which occurred between a Mach number of 0.4 and transonic Mach numbers is indicated in figure 5 to be about the same for all the models, approximately 13-percent chord. At the higher supersonic Mach numbers, however, the aerodynamic centers of the planforms with the cranked leading edges were nearly at the same or slightly ahead of the subsonic positions; whereas the aerodynamic center of the delta planform was considerably behind its subsonic position. At supersonic Mach numbers, the aerodynamic center travel with Mach number for the cranked planforms was, in general, satisfactorily predicted by use of linear theory, but the absolute values for models 5 and 7 were somewhat behind the predicted values. At subsonic Mach numbers the

travel of aerodynamic center with Mach number was not predicted too well by linear theory except for models 1 and 5.

Lift-curve slope $(\partial C_L/\partial \alpha)$.- In figure 6 it can be seen that, in general, at a Mach number of 0.4 and at supersonic Mach numbers, linear theory gave good estimates of the lift-curve slopes except for model 5. At subsonic Mach numbers, however, linear theory gave the proper increase in lift-curve slope with Mach number only for models 1 and 7 and underestimated the increase for the other models. It can also be seen by comparing the experimental values for each model with the values for model 1 (indicated by the circles at three Mach numbers) that the lift-curve slopes for model 1 were either about equal to or greater than those of the cranked planforms.

Drag-due-to-lift factor $(\partial C_D/\partial C_L{}^2)$.- In figure 7 it is interesting to note that at subsonic Mach numbers the measured drag-due-to-lift factors for all planforms with cranked leading edges were considerably below the values predicted by the reciprocal of the lift-curve slope. The latter prediction is known to be a good approximation of the drag-due-to-lift factor for low-aspect-ratio wings with sharp straight leading edges, such as model 1. Evidently, the vortex flow created by the cranked leading edge which produced a lift-curve slope increasing with angle of attack is also favorable in reducing the drag due to lift, even at small angles of attack. Possibly, some leading-edge thrust, not accounted for in theory, is being realized. At supersonic Mach numbers there is reasonable agreement between the measured and predicted drag-due-to-lift factors except for model 5, which has the greatest leading-edge extension. Again, the predicted factors were assumed to be the reciprocal of the lift-curve slopes. The experimental drag-due-to-lift factors for model 1 (indicated by the circles) were either the same or less than those for the cranked planforms.

Minimum drag coefficient (C_{D_o}).- In figure 8 at a Mach number of 0.4 and 1.2 it can be noted that the measured minimum drag of the models with cranked leading edges was less than that for model 1 (the data for which are indicated by the circles). Part of this difference is attributable to less skin friction being measured, as predicted, for the more slender configurations. For example, at a Mach number of 0.4 compare the predicted and measured values for model 7 with corresponding values for model 1. (This effect is discussed in more detail in ref. 4.) At transonic Mach numbers the cranked planforms with rather large leading-edge extensions, such as models 3 through 7, had considerably less minimum drag than the delta planform. At a Mach number of about 3 only the very slender cranked planforms, models 4 through 7, had less drag than the delta planform. The reason that theory and experiment differed so much at the higher Mach numbers for the aspect-ratio-2.2 models is not clearly understood, although it might be expected, intuitively, that the assumption made to compute the wave drag for an "equivalent" body of revolution as described in reference 13 would give better values of drag for the more slender wing-body combinations.

Maximum lift-drag ratio $\left((L/D)_{max}\right)$.- Figure 9 shows that at subsonic Mach numbers all the models with cranked leading edges had considerably higher

lift-drag ratios than predicted. This difference is mainly attributable to the drag due to lift being less than predicted for cranked planforms. At supersonic Mach numbers, linear theory gave good estimates of the measured maximum lift-drag ratios except for model 5. It should be realized, however, that part of this good agreement is fortuitous for some of the models, since compensating effects occurred in the prediction of the minimum drag and the drag due to lift. For model 5 the disagreement between theory and experiment is related to both the minimum drag and the drag due to lift being overpredicted. As indicated by the circles, representing the data for the base model 1, and the curves in figure 9, only models 2, 3, and 6 at a Mach number of 0.4 had slightly higher maximum lift-drag ratios than model 1. At a Mach number of 2.8 only models 5 and 6 had slightly higher maximum lift-drag ratios than model 1.

At the right of each model sketch in figure 9 are shown the volumes of models with cranked planforms relative to that for the model with the delta planform. It should be emphasized that all the wings have nearly the same exposed areas as well as profiles with a thickness of 3-percent chord, constant along the wing spans. The extra volume for the cranked planforms, indicated by the volume ratios being above 1.0, is a result of the cranked planforms having extended chord lengths near the fuselage. Note that model 6 which has 47 percent more volume than the delta wing has measured lift-drag ratios slightly greater than those for the delta wing at the three representative Mach numbers.

Theoretical Potential for L/D by Warping

Results presented in figures 2 through 9 were for models with planar wings which had symmetrical profiles. Recognizing that a final design will be optimized by warping its surface to improve the lift-drag ratio in cruise, two of the models were theoretically warped to determine the gains in efficiency that might accrue. In figure 10 the theoretical lift-drag ratios at flight Reynolds numbers are shown for models 1 and 6, both with and without wing warpage. In the calculations the following flight conditions were assumed: A Mach number of 3.0, an altitude of 70,000 feet, a design lift coefficient of 0.07, and a wing area of 9970 sq ft. The theoretical increments in lift-drag ratio due to warping were calculated by the method of reference 14 which gives the optimum cambered wing surface and associated pressure drag. For the flat wings, the lift-drag ratios are those obtained by extrapolating the experimental values to the flight Reynolds number for a given wing-body combination at the chosen lift coefficient and Mach number. The decrement of skin-friction drag due to the increase in Reynolds number was obtained by the method of reference 10. It can be seen that even the flat version of model 6 has a considerably higher lift-drag ratio than the model with the delta wing. Also, it is evident that the delta wing with a supersonic leading edge gains little in lift-drag ratio from warping; however, model 6, with part of its leading edge subsonic, theoretically can have about a 10-percent improvement in its lift-drag ratio.

CONCLUDING REMARKS

It has been shown that wing-body combinations employing planforms with cranked leading edges can be designed to have the same aerodynamic center at high supersonic and subsonic Mach numbers. At subsonic Mach numbers these cranked planforms had considerably less drag due to lift, and consequently higher lift-drag ratios, than was predicted from linear theory, although these planforms also exhibited a loss in longitudinal stability. For the same exposed area and thickness in percent chord, cranked planforms have more usable volume yet less minimum drag than delta planforms. At a Mach number of 3.0, it has been shown that some cranked planforms not only have considerably higher lift-drag ratios than their straight leading-edge counterparts when planar wings are used but also these planforms have more theoretical potential for improvements in flight efficiency by warping.

REFERENCES

1. Hicks, Raymond M.; and Hopkins, Edward J.: Effects of Spanwise Variation of Leading-Edge Sweep on the Lift, Drag, and Pitching Moment of a Wing-Body Combination at Mach Numbers From 0.7 to 2.94. NASA TN D-2236, 1964.

2. Robins, A. Warner; Harris, Roy V., Jr.; and Jackson, Charlie M., Jr.: Characteristics at Mach Number of 2.03 of a Series of Wings Having Various Spanwise Distributions of Thickness Ratio and Chord. NASA TN D-631, 1960.

3. Shrout, Barrett L.: Zero-Lift Drag at Mach 1.42, 1.83, and 2.21 of a Series of Wings With Variations of Thickness Ratio and Chord. NASA TN D-2811, 1965.

4. Hopkins, Edward J.: Some Effects of Planform Modification on the Skin Friction Drag. AIAA J. (Tech. Comments), vol. 2, no. 2, Feb. 1964, pp. 413-414.

5. Pitts, William C.; Nielsen, Jack N.; and Kaattari, George E.: Lift and Center of Pressure of Wing-Body-Tail Combinations at Subsonic, Transonic, and Supersonic Speeds. NACA Rept. 1307, 1957.

6. Lomax, Harvard; and Sluder, Loma: Chordwise and Compressibility Corrections to Slender-Wing Theory. NACA Rept. 1105, 1952. (Supersedes NACA TN 2295.)

7. DeYoung, John; Rule of Thumb Equation for Predicting Lifting-Surface-Theory Values of Lift. J. Aeron. Sci., (Readers' Forum), vol. 24, no. 8, Aug. 1957, p. 629.

8. DeYoung, John, and Harper, Charles W.: Theoretical Symmetric Span Loading at Subsonic Speeds for Wings Having Arbitrary Plan Form. NACA Rept. 921, 1948.

9. Schlichting, Hermann, (J. Kestin, trans.): Boundary Layer Theory. McGraw-Hill Book Co., Inc., 1955, p. 540.

10. Sommer, Simon C.; and Short, Barbara J.: Free-Flight Measurements of Turbulent-Boundary-Layer Skin Friction in the Presence of Severe Aerodynamic Heating at Mach Numbers From 2.7 to 7.0. NACA TN 3391, 1955.

11. Woodward, F. A.: A Method of Aerodynamic Influence Coefficients With Application to the Analysis and Design of Supersonic Wings. Doc. D6-8178, The Boeing Co., April 1962.

12. Middleton, Wilbur D.; and Carlson, Harry W.: A Numerical Method for Calculating the Flat-Plate Pressure Distributions on Supersonic Wings of Arbitrary Planform. NASA TN D-2570, 1965.

13. Harris, Roy V., Jr.: An Analysis and Correlation of Aircraft Wave Drag. NASA TM X-947, 1964.

14. Woodward, F. A., and Larson, J. W.: Staff of the Aerodynamic Research Unit. A Method of Optimizing Camber Surfaces For Wing-Body Combinations at Supersonic Speeds. Part I. - Theory and Application. Doc. D6-10741, Pt. I, (Prepared for NASA under contract no. NAS2-2282.) The Boeing Co., 1965.

MODEL GEOMETRY

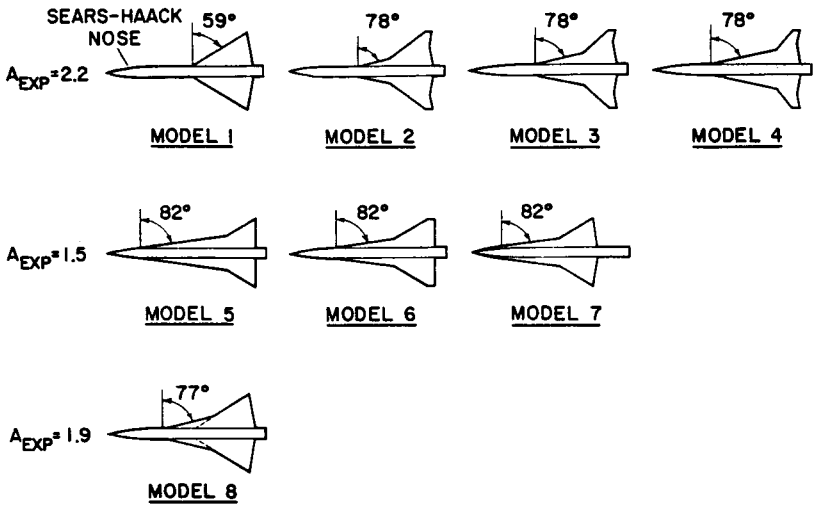

Figure 1

REYNOLDS NUMBER EFFECTS

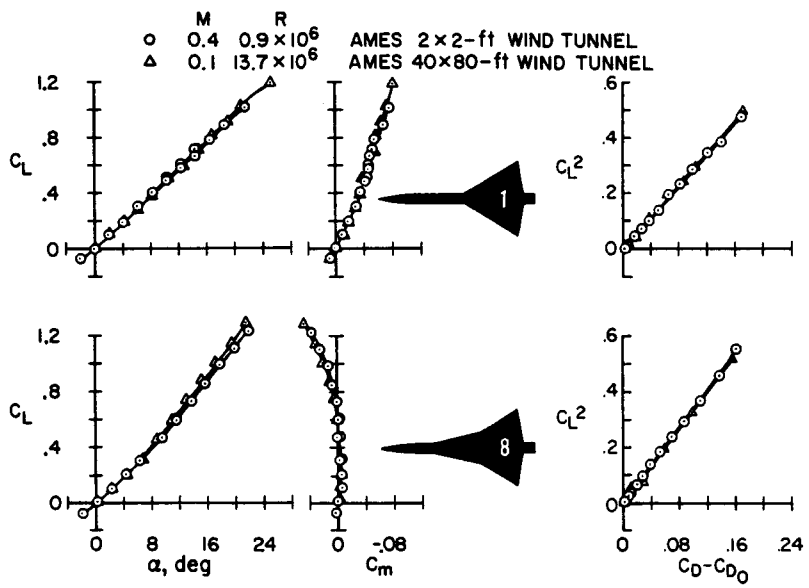

Figure 2

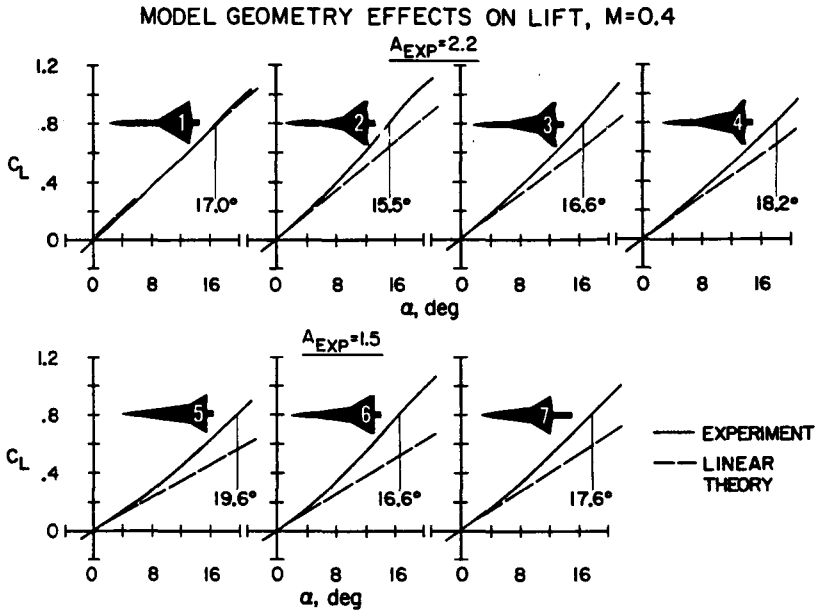

Figure 3

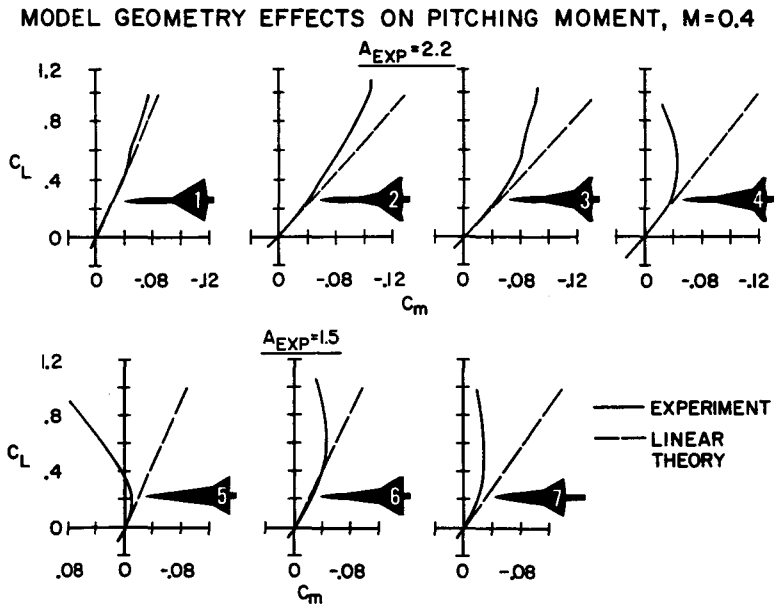

Figure 4

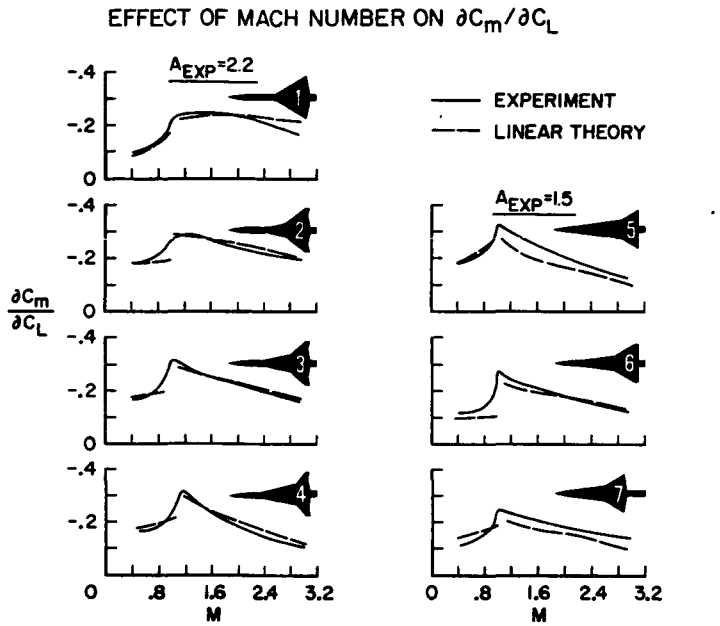

Figure 5

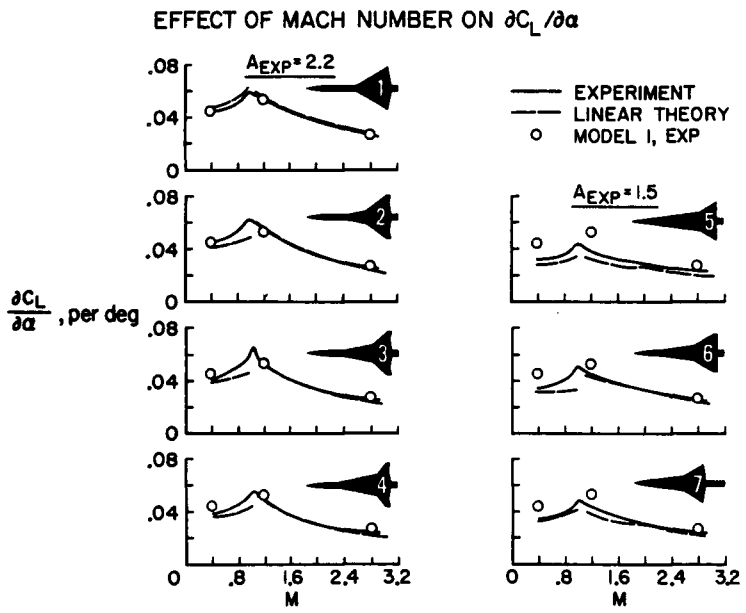

Figure 6

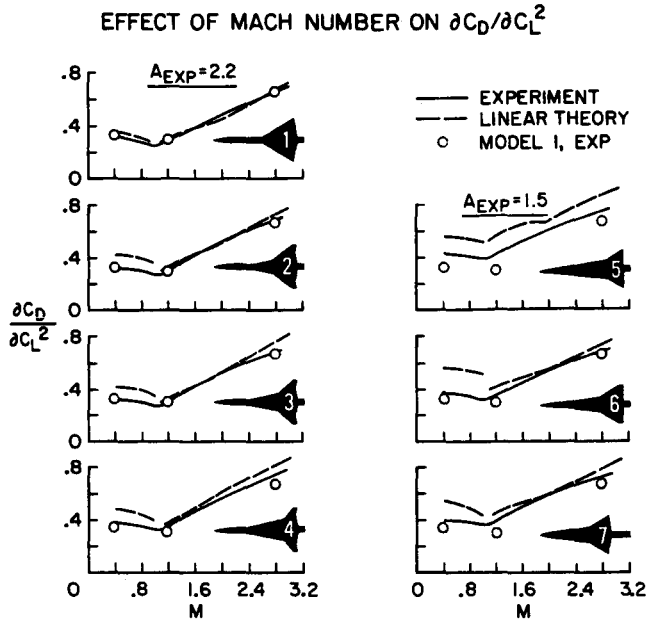

Figure 7

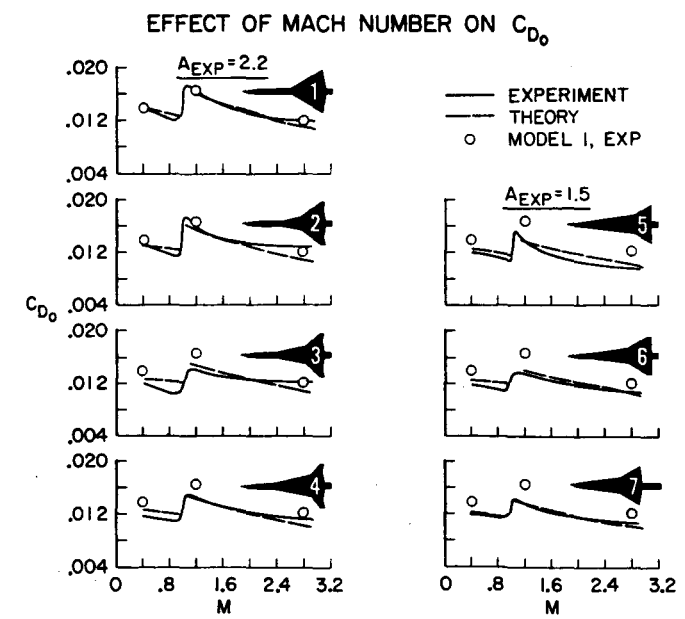

Figure 8

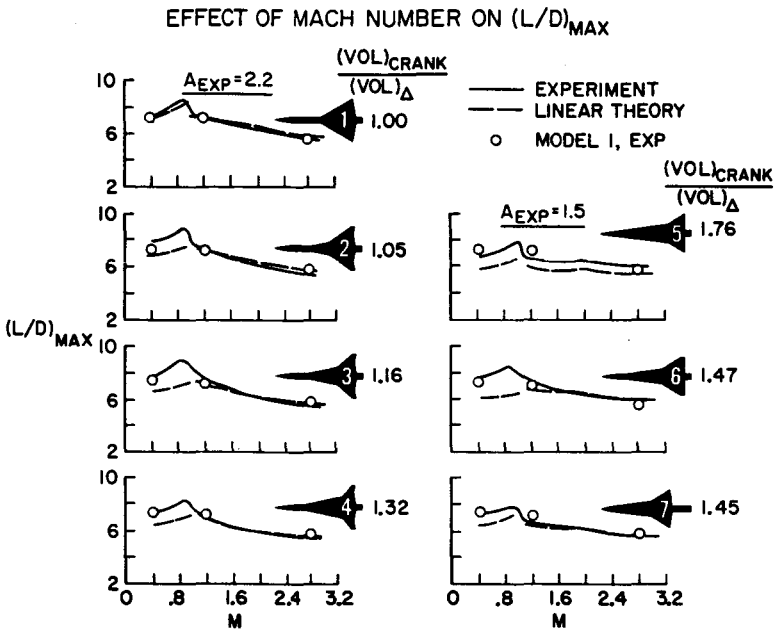

Figure 9

THEORETICAL POTENTIAL FOR L/D OF MODELS I AND 6

ASSUMED FLIGHT CONDITIONS:

- M = 3
- 70,000 ft
- S = 9,970 ft^2
- C_L = .07

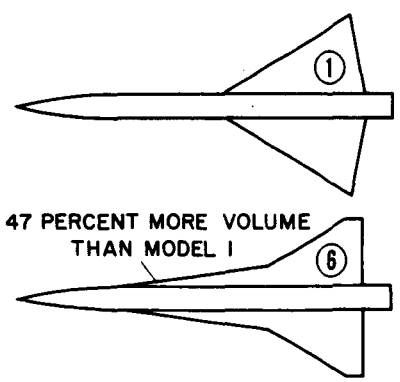

L/D FLAT WING	L/D WARPED WING
6.80	6.85
7.60	8.47

Figure 10